Plasma Chemistry and Plasma Processing, Vol. 4, No. 1, 1984

Radiofrequency Plasma Decomposition of C_nF_{2n+2}–H_2 and CF_4–C_2F_4 Mixtures During Si Etching or Fluoropolymer Deposition

Riccardo d'Agostino,[1] Santolo De Benedictis,[1] and Francesco Cramarossa[1]

Received February 10, 1983; revised June 22, 1983

Microscopic decomposition processes and gas–solid interactions in C_nF_{2n+2}–H_2 and CF_4–C_2F_4 discharges are studied by comparing mass-spectrometric results with actinometric emission diagnostics. The role played by CF_x radicals is evident in the various processes of gas-phase formation of saturates and unsaturates as well as in the "activation growth mechanism" of polymer deposition.

KEY WORDS: Silicon etching; polymerization of fluorocarbons; plasma decomposition of fluorocarbons.

1. INTRODUCTION

A great deal of work has recently been done in the field of gas-phase plasma diagnostics with the aim of understanding the role played by unstable and stable species produced in radiofrequency discharges of fluorocarbons during the processes of plasma fluoropolymer film deposition and plasma etching for fine lithography techniques. Among the various diagnostic techniques, mass spectrometry[1] and emission spectroscopy[2–6] proved to be the most promising tools for monitoring active species.

Very recently a new diagnostic technique, which makes use of "actinometer" gases, has been demonstrated by Coburn *et al.*[7,8] and d'Agostino *et al.*[9–14] The technique consists essentially in adding, to the feed, actinometric gases such as N_2, Ar, or He, and in following their emissions at 380.5, 750.3, and 587.5 nm, respectively, in order to determine

[1] Centro di Studio per la Chimica dei Plasmi del C.N.R., Dipartimento di Chimica dell'Università, Via Amendola, 173, 70126, Bari, Italy.

0272-4324/84/0300-0001$03.50/0

the electron excitation functions. A combination of the excitation efficiency of the emitting levels of the actinometric gases with the emission intensities of some species allows the determination of the variation of the ground-state species densities with plasma parameters (feed compositions, power input, etc.). The validity and applicability limits of the technique have been examined in numerous works.[10–18] This technique has been utilized by us to explain and classify the properties of discharges fed with fluorocarbons, and to examine their decomposition channels.[12] It has also been utilized to investigate the microscopic interactions between CF_x radicals, F atoms and electrons, and silicon or fluoropolymer surfaces, during Si etching or polymer deposition on it, when C_nF_{2n+2}–H_2 (or C_2F_4) mixtures are used, under conditions identical to those of the present work.[13]

In this note we compare the results obtained by mass-spectrometry with those obtained by emission actinometric spectroscopy (actinometry) in order to clarify the decomposition channels of perfluorocarbons (C_nF_{2n+2}) in the presence of reducing agents (H_2, C_2F_4) and to ascertain the validity of actinometry for evaluating microscopic etching and polymerization mechanisms. The results obtained, confirming the activation growth mechanism of polymer deposition and the Si etching by F atoms, allow us to suggest a simplified microscopic model of discharge processes, which involves CF_x radicals and which accounts for the observed trends of the various stable and unstable species, and for the polymerization rates as a function of the discharge parameters.

2. EXPERIMENTAL

A schematic drawing of the apparatus, which has been described in detail elsewhere,[9,10] is shown in Fig. 1. The tubular reactor (1.8 cm i.d., 50 cm length) was made of alumina and capacitively coupled to a 27-MHz generator by means of two external brass electrodes (5 × 5 cm). The experiments were carried out under the following conditions: pressure = 0.5 torr, power input = 50 W, total gas flow rate = 50 sccm. Details for the spectroscopic measurements are reported in Refs. 9, 12, and 13 along with the criteria for the actinometric analysis of the density trends of F atoms, CF and CF_2 radicals, and the electron excitation function for the various C_nF_{2n+2}–H_2, C_2F_4 mixtures examined. Values of Si etching and polymerization rates have been determined gravimetrically. The experiments have been carried out with (111) substrates lying over an Al_2O_3 plate immersed in the discharge and facing the potential electrode. With this configuration of substrate holder decoupled from ground, the substrate is kept at a potential close to that of the plasma, and ion collisions should give a low contribution to charged particle bombardment of the substrate because at

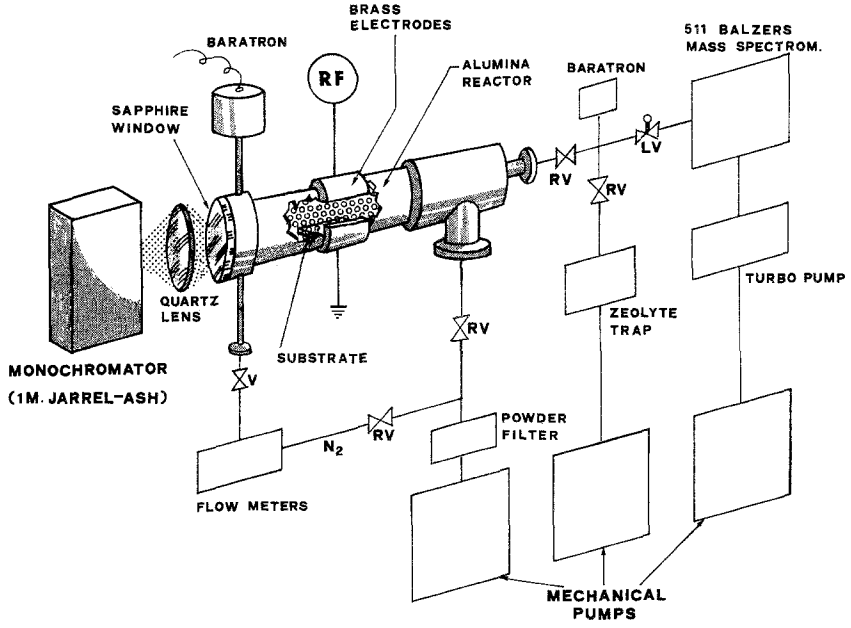

Fig. 1. Experimental apparatus. (RV) Regulating valves; (V) valves; (LV) leak valve.

27 MHz and 0.5 torr ions would not be able to follow the applied field and would move only by diffusion.

The discharge products, sampled through a leak valve in the sampling system shown in Fig. 1, entered the ionization chamber where they were ionized by 20-eV electrons, and the positive ions produced were then mass-analyzed in a Balzers type QMG 511 quadrupole equipped with a 250 liter sec^{-1} turbomolecular pump. The ionization energy of 20 eV was chosen in order to reduce fragmentation and the degree of reactions among the various fragments, to identify heavier compounds such as C_3, C_4, C_5, and C_6 fluorocarbons, and also to reduce the fragmentation of unsaturated compounds such as C_2F_4. The pressure in the ionization chamber was kept in the range of $5 \cdot 10^{-6}$ to 10^{-5} torr, and the mass spectra of the discharge effluents were always compared with the spectra obtained with the discharge off.

In Fig. 2 we report the predominant mass peaks obtained with pure C_2F_4 under both conditions: discharge on and discharge off. It can be seen that, with the present analysis conditions (chamber pressure 10^{-5} torr, 20 eV), the ion peaks arising from C_2F_4 fragmentation in the quadrupole are $C_2F_4^+$ ($m/e = 100$), $C_2F_3^+$ ($m/e = 81$), CF_2^+ ($m/e = 50$), and CF^+ ($m/e = 31$), while CF_3^+ ($m/e = 69$), $C_3F_5^+$ ($m/e = 131$), and $C_3F_6^+$ ($m/e = 150$) are

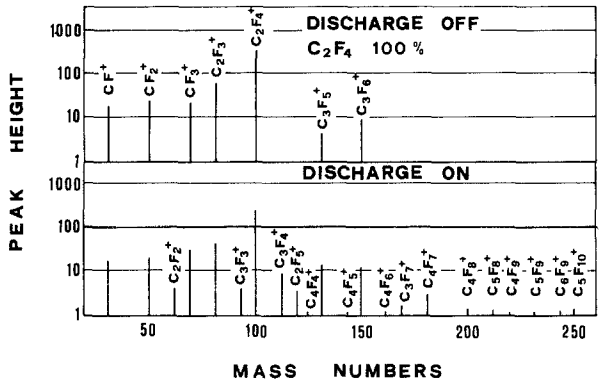

Fig. 2. Main mass peaks from pure C_2F_4.

the result of reactions in the mass chamber between the fragments and C_2F_4. A comparison of these spectra with those obtained with the discharge on shows that many saturates and unsaturates are formed, even with numbers of carbon atoms as high as 6. The results obtained with different mixtures indicate that reactions of fragments in the mass chamber are negligible.

Argon fed into the mixture at constant small flow (about 1%) was utilized both as actinometric gas for emission spectroscopy and as mass-spectrometric internal standard in order to compare results under different conditions. The rotary pump utilized for evacuating the sampling chamber was equipped with a zeolite trap to prevent back-streaming of pump oil. The rotary pump used for the flowing system was equipped with Fomblin L Vac 16 oil (a perfluorinated polyether manufactured by Montedison) to prevent corrosion and damaging of the pump. Dry nitrogen was utilized as ballast gas both to reduce the partial pressure of corrosive agents in the pump and to prevent hydrolysis of the products in the exhaust stream at the end of each run. The pumping system has been operated for more than a year without any alteration of the pumping performances.

3. THE EFFECT OF REDUCING AGENTS ON C_nF_{2n+2} DECOMPOSITION

3.1. Conversion Trends

Reducing agents such as H_2, or unsaturated fluorocarbons such as C_2F_4, or the silicon itself, behave as F-atom scavengers and lead to the formation of either HF, saturates such as C_2F_6, or etching products such as SiF_4. The

depletion of F atoms reduces the recombination reactions:

$$F + CF_x \rightarrow CF_{x+1} \qquad (x = 0\text{–}3) \tag{1}$$

and does not affect processes such as

$$CF_x \rightarrow CF_{x-1} + F \qquad (x = 4\text{–}1) \tag{2}$$

$$CF_x + CF_x \rightarrow CF_{x+1} + CF_{x-1} \qquad (x = 3\text{–}1) \tag{3}$$

This leads to a net increase of CF_x radicals in the gas phase.[12] The change of the $[CF_x]/[F]$ ratio in the gas phase leads to a variation of the plasma medium characteristics, since HF, C_2F_6, and SiF_4 are very poor etchants with respect to F atoms, while CF_x radicals can lead to the following processes:

(i) etching of SiO_2, which can increase the SiO_2/Si etching selectivity;[19–21]

(ii) polymerization over a silicon surface, provided enough active sites are created by charged particles on the polymer surface to assist the growing process;[13]

(iii) reactions with gas-phase unsaturated and saturated species[22,23] which lead to higher chain compounds such as C_3–C_6 fluorocarbons.

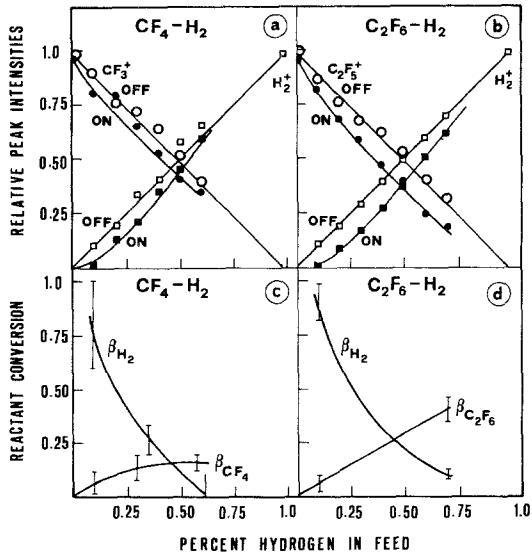

Fig. 3. Relative peak intensities with discharge on and off and conversions of reactants, β, in CF_4–H_2 and C_2F_6–H_2 as a function of percent hydrogen in feed.

In Fig. 3a and 3b the overall effect of introducing H_2 in the feed is shown for CF_4 and C_2F_6. In this figure the results are compared with those obtained with the discharge off, and the relative decrease of the ions peaks (CF_3^+, $m/e=69$, $C_2F_5^+$, $m/e=119$, H_2^+, $m/e=2$), which is due to the reactions caused by the discharge, can be assumed proportional to the overall (CF_4, C_2F_6, and H_2) reactant conversions in the various mixtures.

It can be seen from these figures that the relative decrease of CF_3^+ and $C_2F_5^+$ peaks follows approximately the same trends and that the discharge activation for hydrogen, i.e., the relative decrease of the H_2 peak, is higher the lower the hydrogen percentage in the feed. In Fig. 3c and 3d the overall reactant conversions have been plotted as a function of the percent hydrogen in the feed for both cases. It can be seen that at low hydrogen compositions almost all of it reacts with fluorocarbons, while its conversion decreases with increasing reactant availability in the feed. On the contrary, the overall fluorocarbon conversion increases with increasing H_2 in the feed; this effect is more pronounced in C_2F_6 than in CF_4, where a tendency toward a maximum conversion of ~18% is shown at ~50% H_2 in the feed.

In Fig. 4 the trends of the ion peak $C_2F_4^+$ ($m/e=100$) has been reported for CF_4–C_2F_4 mixtures, for both discharge on and off. In this case we cannot use as a diagnostic species the CF_3^+ ($m/e=69$) peak because this ion is generated also in the spectrometer chamber in the presence of high amounts of CF_2^+ and/or CF_2 and F, as for C_2F_4-rich effluents (see Fig. 2). The profiles of $C_2F_4^+$ reveal high conversions of C_2F_4 into products when it is in mixture with CF_4, and also as a pure feed.

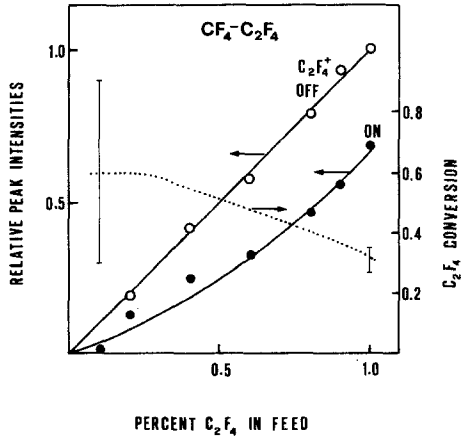

Fig. 4. Relative peak intensities of C_2F_4 parent ion with discharge on and off and C_2F_4 conversion as a function of percent C_2F_4 in feed for CF_4–C_2F_4 mixtures.

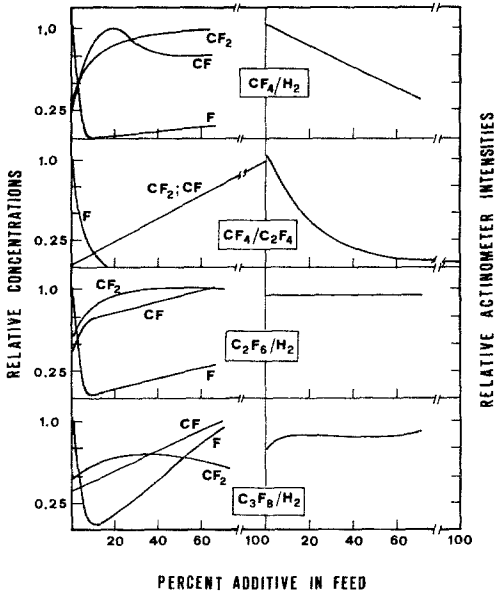

Fig. 5. Emission actinometric results of Ref. 13: relative concentrations of F atoms and CF_x radicals and relative emissions of both actinometers (N_2 and Ar) as a function of percent additive in feed.

The low accuracy of the conversion data, particularly at lower C_2F_4 percentages, does not hinder the conversion trend, which smoothly decreases with increasing C_2F_4 content in the mixture. The differences from the steeper decrease observed for hydrogen conversions in C_nF_{2n+2}–H_2 mixtures are the result of three effects caused by the addition of C_2F_4:

(1) the linear increase of both CF and CF_2 radicals (see Fig. 5);
(2) the decrease of CF_4 concentration;
(3) the marked decrease of electron density.

Points (1) and (3) will be discussed later.

3.2. Trends of Active Species

The results shown in Figs. 3 and 4 should be explainable on the basis of actinometry with the data reported in Fig. 5 which have been taken from Ref. 13. In CF_4–H_2 mixtures, CF_2 concentration is a maximum at about 50% H_2, and CF radicals exhibit an earlier maximum, while in C_2F_6–H_2, CF_2 has about the same trend but CF always increases. A similar trend for CF_2 and CF is found for C_3F_8–H_2 mixtures, while for CF_4–C_2F_4 mixtures

both radicals increase linearly with C_2F_4 percentage in the feed. Tetrafluoroethylene is in fact a source of CF_x radicals, and this leads to the formation in the discharge of various "addition" compounds such as C_2–C_6 compounds.

In Fig. 5 trends of the emission intensities of both actinometers are also reported. These emissions are related to the electron excitation function, $f(n_e)$, a function of the electron densities, n_e, at energies $E \geq E_{th}$ (where E_{th} is 11.5 and 13.7 eV for N_2 and Ar, respectively). The observed coincidence of the trends for the two actinometric gases is an indication that, under our experimental conditions, $f(n_e)$ is independent of the excitation cross sections, and therefore the emission intensity trends can be assumed proportional to the electron density in a broad energy range.[13] With this assumption, it can be observed that C_2F_4 acts as a sink of fast electrons; in fact their density decreases almost exponentially in the CF_4–C_2F_4 plasma on C_2F_4 addition, while a linear decrease is observed in CF_4–H_2, and an almost independent behavior in C_2F_6–H_2 and C_3F_8–H_2 mixtures.

3.3. Trends of End Products

In Fig. 6 the normalized peak intensities of HF^+ ($m/e = 20$) and $C_2H_2^+$ ($m/e = 26$) are plotted as a function of the hydrogen percentage in the feed for CF_4–H_2 mixtures. The narrow maximum of the HF^+ peak is related to the minimum in the fluorine atom density, shown in Fig. 5, and the increasing hydrogen concentration (see Fig. 3). The decrease in HF^+ intensity after the maximum is too steep to be explained only on the basis of the dilution caused by H_2 addition. This result seems to confirm the hypothesis of F-atom re-formation with increase in the H content, as suggested by an analysis of

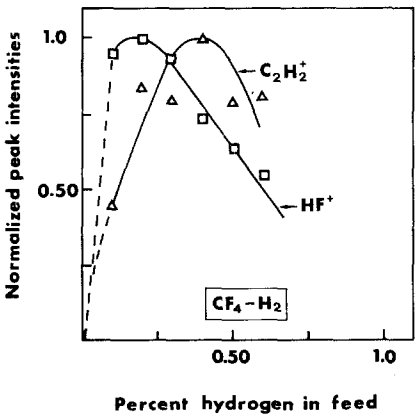

Fig. 6. Normalized peak intensities of C_2H_2 and HF parent ions vs. percent hydrogen in feed in CF_4–H_2 discharges.

the "actinometric" results in Ref. 13, on the basis of the two possible reactions:

$$HF + e \rightarrow H + F + e \tag{4}$$

$$H + HF^{\ddagger} \rightarrow H_2 + F \tag{5}$$

where $HF^{\ddagger}$ refers to vibrationally excited HF, which is always present in large amounts when hydrogen is added to fluorine-containing discharges.[24] The first reaction should probably give only a minor contribution to F-atom re-formation, at least in CF_4–H_2 where the actionometer's density trend, and probably the electron density, decrease with hydrogen addition. F atom re-formation is observed in all C_nF_{2n+2}–H_2 mixtures.

In Fig. 7 the HF^+ trend in C_2F_6–H_2 mixtures is shown, along with the trends of $C_2H_2^+$ and $C_2F_4^+$ ($m/e = 100$), which are quite similar to that observed for CF_4–H_2. A completely different behavior is observed for the $C_2H_2^+$ peak: while it always increases with hydrogen content in C_2F_6–H_2, it shows a clear maximum in CF_4–H_2. This is probably due to a different electron density behavior. In fact, a decrease in the electron density and/or electron distribution function reduces the rate of the primary decomposition channel[12]

$$CF_4 + e \rightarrow CF_3 + F + e \tag{6}$$

and the rate of reaction of fragments with both H and H_2.

It can also be seen from Fig. 7 that the $C_2F_2^+$ peak intensity increases with H_2 in the feed in a very similar way to that observed spectroscopically for CF_2 radicals (see Fig. 5). These similarities are in agreement with the general consensus on the role of unsaturates such as C_2F_4 or C_2F_2 as sources of CF_2 and CF radicals,[23–25] respectively. The rapid raction rates involved

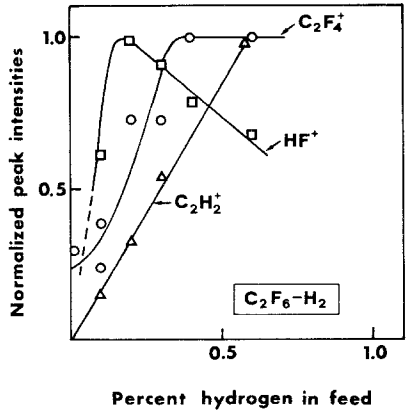

Fig. 7. Normalized peak intensities of C_2H_2, HF, and C_2F_4 parent ions vs. percent hydrogen in C_2F_6–H_2 discharges.

in the plasma phase[12] should lead to the "plasma-chemical equilibria"

$$C_2F_4 \rightleftharpoons CF_2 + CF_2 \tag{7}$$

$$C_2F_2 \rightleftharpoons CF + CF \tag{8}$$

The correspondence between radical concentrations determined by actinometry and "end-products" by mass-spectrometric analysis emerges by comparing the data of Fig. 5 with those of Fig. 8, where mass peak intensities corresponding to $C_2F_2^+(C_2F_2)$, $C_3F_3^+$, $C_2F_5^+(C_2F_6)$, $C_3F_4^+(C_3F_4)$, $C_3F_6^+(C_3F_6)$, and $C_3F_7^+(C_3F_8)$ are reported vs. C_2F_4 percentage in CF_4–C_2F_4 mixtures. CF_x radicals (see Fig. 5) and C_2F_4 densities (see Fig. 4) increase almost linearly with C_2F_4 addition, while CF_4 decreases. On the basis of these trends, one should expect that: (a) species originating from the rapid recombination reactions between radicals ($CF_x + CF_x$) and/or between radicals and C_2F_4 ($CF_x + C_2F_4$) should increase almost linearly with C_2F_4 addition; (b) species originating from the recombination between CF_4 and either CF_x radicals or C_2F_4 (both $CF_4 + CF_x$ and $CF_4 + C_2F_4$ processes)

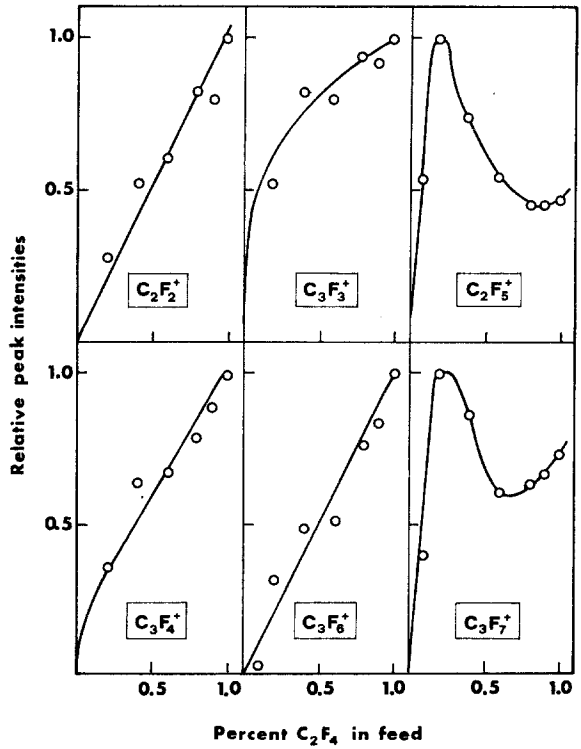

Fig. 8. Normalized peak intensities of various ions vs. C_2F_4 percentage in CF_4–C_2F_4 mixtures.

should show a maximum with C_2F_4 addition. Points (a) and (b) hold provided that recombination processes are faster than their respective decomposition reactions. These trends are clearly seen in Fig. 8:

—$C_2F_2^+$, which is related to fluoroacetylene, increases linearly with C_2F_4 addition, as would be expected from the linear increase of CF radicals in Fig. 5;

—$C_2F_5^+(C_2F_6)$, originating from the fast equilibrium reaction $CF_4 + CF_2 \rightleftharpoons C_2F_6$, goes through a maximum, this finding is in perfect agreement with the results shown in Ref. 12, where this fast reaction has been assumed as the main decomposition channel prevailing with respect to $C_2F_6 \rightleftharpoons CF_3 + CF_3$ in C_2F_6 discharges;

—$C_3F_7^+$, which comes out from C_3F_8, shows the same profile as $C_2F_5^+$ and should originate from either of the direct recombinations $CF_4 + C_2F_4 \rightarrow C_3F_8$ or $CF_4 + CF_2 + CF_2 \rightarrow C_3F_8$;

—$C_3F_6^+$, corrected for the contributions arising from recombinations in the mass chamber (Fig. 2), also shows a linear relationship with C_2F_4 addition; in fact, its production should occur through $CF_2 + C_2F_4 \rightarrow C_3F_6$;

—similar considerations should apply to explain the $C_3F_4^+$ and $C_3F_3^+$ trends, even though the interpretation would be more speculative at the moment.

4. DISCHARGE MECHANISMS

The experimental results reported allow us to correlate the formation of end products, such as HF and various saturates and unsaturates, with the main "active" species, namely F atoms, CF_x radicals, and electrons. In a previous paper d'Agostino *et al.*[13] have shown that etching and polymerization rates can also be correlated through detailed mechanisms to the concentration trends of the same active species. A general simplified mechanism can now be suggested which accounts for the various macroscopic parameters in C_nF_{2n+2}–(H_2 or C_2F_4) discharges on the basis of the possible microscopic processes.

In Ref. 13 it has been found that F atoms etch silicon without any help by charged particles or without competing with other species which could cover active sites, provided that substrates are uncoupled from ground and that the $[F]/[CF_x]$ ratio is high.

In this case accurate predictions of the silicon etch rate are possible because it is directly proportional to the F atom concentration and independent of the feeds utilized. On the other hand, it has been found that polymer deposition can occur by direct gas-phase radical deposition over surface

sites of the polymer previously activated (activation growth model, AGM) by impact with charged particles of low energy. The corresponding polymer deposition rate for the AGM has been written[13] as

$$r_p = A\frac{[R_g]f(n_e)}{[M]} \tag{9}$$

where A is constant, $[R_g]$ and $[M]$ are the concentrations of radicals and neutrals, and $f(n_e)$ is the electron excitation function, a function of the electron density. Equation (9) reproduces the experimental deposition rates in the various mixtures fairly well, as shown in Ref. 13, and is the first tentative *direct* experimental correlation of external and internal parameters in fluoropolymer deposition discharges. The real importance of low-energy charged particle bombardment, i.e. of $f(n_e)$ in Eq. (9), in this type of polymerization discharge can be fully realized by comparing Fig. 8 with Fig. 4 of Ref. 13. It can be seen that, by increasing the reducing agent (C_2F_4) in the feed, the production of heavier C_2–C_6 compounds increases through CF and CF_2 radical recombination with both stable and unstable compounds. However, heavier compounds cannot be regarded as intermediates in the polymer deposition, as generally believed[25–27]: it is found that polymer deposition rates go through a maximum at 30% C_2F_4, as a consequence of the decrease of $f(n_e)$ (see Fig. 5), while the production of C_2–C_6 addition compounds generally increases with C_2F_4 addition. A simplified model of mechanisms that take into account the various phenomena occurring both in the gas phase and on the surface in fluoropolymerization discharges is

$$e + C_nF_{2n+2} + H_2 \text{ or unsaturates} \xrightarrow[\text{activation}]{\text{plasma}} e + CF_x + HF \text{ or saturates} \tag{10}$$

$$CF_x + CF_x, \text{ unsaturates or saturates} \rightarrow C_2\text{–}C_6 \text{ addition compounds} \tag{11}$$

$$CF_x + (Pol)_n^* \rightarrow (Pol)_{n+1}^* \tag{12}$$

$$\left\{\begin{matrix} e \\ I^-, I^+ \end{matrix}\right\} + (Pol)_n \rightarrow (Pol)_n^* \tag{13}$$

$$M + (Pol)_n^* \rightarrow (Pol)_n + M \tag{14}$$

Reaction (10) of the model represents the creation of CF_x species, i.e., the building blocks for both addition compounds [stage (11)] and polymer deposition on "activated" surface sites [stage (12)]. Stages (13) and (14) take into account activation through charged particle bombardment and

deactivation through neutral interactions, respectively. Activated sites are denoted by asterisks.

5. CONCLUSION

The use of different approaches, such as actinometry and mass spectrometry, to discharges utilized for etching and/or polymerization with perfluorinated hydrocarbons in mixtures with other additives largely enhances the diagnostic possibilities in elucidating etching and polymer formation mechanisms. Macroscopic parameters, such as etch and polymer deposition rates, as well as production of stable compounds, can be correlated *directly* to the relevant microscopic processes through the density trends of radicals and atoms.

REFERENCES

1. G. Smolinsky and D. L. Flamm, *J. Appl. Phys.* **50**, 4982 (1979); E. Kay, A. Dilks, and D. Seybold, *J. Appl. Phys.* **51**, 3678 (1980).
2. W. R. Harshbarger, T. A. Miller, P. Norton, and R. A. Porter, *Appl. Spectrosc.* **31**, 201 (1977).
3. C. J. Mogab, A. C. Adams, and D. L. Flamm, *J. Appl. Phys.* **49**, 3796 (1978).
4. W. R. Harshberger, R. A. Porter, and P. Norton, *J. Electron. Mater.* **7**, 429 (1978).
5. B. J. Curtis and H. J. Brunner, *J. Electrochem. Soc.* **125**, 829 (1978).
6. R. Gilbert, J. Castonguay, and A. Théorêt, *Can. J. Spectrosc.* **25**, 15 (1980).
7. J. W. Coburn and M. Chen, *J. Appl. Phys.* **51**, 3134 (1980).
8. J. W. Coburn and M. Chen, *J. Vac. Sci. Technol.* **18**, 353 (1981).
9. R.d'Agostino, F. Cramarossa, S. De Benedictis, and G. Ferraro, *J. Appl. Phys.* **52**, 1259 (1981).
10. R. d'Agostino, V. Colaprico, and F. Cramarossa, *Plasma Chem. Plasma Process.* **1**, 365 (1981).
11. R. d'Agostino, V. Colaprico, and F. Cramarossa, *Proceedings of the 5th International Symposium on Plasma Chemistry* (ISPC-5), Vol. 1, Edinburgh (1981), p. 25; R. d'Agostino, V. Colaprico, and F. Cramarossa, *Proceedings of the XIV Congresso Nazionale di Chimica Inorganica*, F13, Torino (1981).
12. R. d'Agostino, F. Cramarossa, and S. De Benedictis, *Plasma Chem. Plasma Process.* **2**, 213 (1982).
13. R. d'Agostino, F. Cramarossa, V. Colaprico, and R. d'Ettole, *J. Appl. Phys.* **54**, 1284 (1983).
14. C. Gorse, S. De Benedictis, M. Cacciatore, M. Capitelli, F. Cramarossa, and R. d'Agostino, *Proceedings of the XV Congresso Nazionale di Chimica Inorganica*, F6, Bari (1982).
15. H. J. Tiller, D. Berg, and R. Mohr, *Plasma Chem. Plasma Process.* **1**, 247 (1981).
16. H. Sabadil and M. Hannemann, *Proceedings of the 5th International Symposium on Plasma Chemistry* (ISPC-5), Vol. 2, Edinburgh (1981), p. 498.
17. C. Gorse *et al.*, to be published.
18. D. L. Flamm, V. M. Donnelly, R. H. Bruce, and G. J. Collins, *Proceedings of the 5th International Symposium on Plasma Chemistry* (ISPC-5), Vol. 1, Edinburgh (1981), p. 307; D. L. Flamm *et al.*, to be published.

19. R. Heinecke, *Solid State Electron.* **18**, 1146 (1975).
20. R. Heinecke, *Solid State Electron.* **19**, 1039 (1976).
21. E. Kay, J. Coburn, and A. Dilks, in *Topics in Current Chemistry: Plasma Chemistry III*, D. Veprek and M. Venugopalan, eds., Springer, Berlin (1980), p. 1.
22. D. L. Flamm, *Plasma Chem. Plasma Process.* **1**, 37 (1981).
23. D. L. Flamm, P. L. Cowan, and J. A. Golovchenko, *J. Vac. Sci. Technol.* **17**, 1341 (1980).
24. L. Bertrand, H. J. Cagne, R. G. Bosisio, and M. Naisau, *IEEE J. Quantum Electron.* **14**, 8 (1978); O. D. Krogh and G. C. Pimentel, *J. Chem. Phys.* **67**, 2993 (1977).
25. E. Kay and A. Dilks, *Thin Solid Films* **78**, 309 (1981).
26. E. Kay and A. Dilks, *J. Vac. Sci. Technol.* **18**, 1 (1981).
27. M. M. Millard and E. Kay, *J. Electrochem. Soc.* **129**, 160 (1982).